

Optimal gauge for the multimode Rabi model in circuit QED

Marco Roth,^{1,2} Fabian Hassler,² and David P. DiVincenzo^{1,2}

¹JARA Institute for Quantum Information (PGI-11),
Forschungszentrum Jülich, 52428 Jülich, Germany

²JARA-Institute for Quantum Information, RWTH Aachen University, 52056 Aachen, Germany
(Dated: April 2019)

In circuit QED, a Rabi model can be derived by truncating the Hilbert space of the anharmonic qubit coupled to a linear, reactive environment. This truncation breaks the gauge invariance present in the full Hamiltonian. We analyze the determination of an optimal gauge such that the differences between the truncated and the full Hamiltonian are minimized. Here, we derive a simple criterion for the optimal gauge. We find that it is determined by the ratio of the anharmonicity of the qubit to an averaged environmental frequency. We demonstrate that the usual choices of flux and charge are not necessarily the preferred options in the case of multiple resonator modes.

Circuit QED [1, 2] is a central subject of quantum information science that has deepened our understanding of light-matter interaction [3–5]. Most implementations consist of a two-level system (qubit) that is coupled to a linear environment. The qubit is formed by the two lowest energy levels of an anharmonic multilevel-system. For the physics of interest only the qubit subspace is important. The Schrieffer-Wolff (SW) transformation [6, 7] is the standard method to perturbatively derive an effective Hamiltonian description within this subspace. For most purposes, it is sufficient to consider the effective Hamiltonian only to first order, yielding the well known quantum Rabi model (QRM). However, since the Hamiltonian of the non-truncated system is unique only up to a unitary transformation, the effective description is gauge dependent to every finite order [8, 9]. This gauge ambiguity becomes particularly important in the (ultra) strong coupling regime. It has been found that the QRM derived in a gauge where the qubit-resonator coupling is mediated by the flux variables leads to different predictions than the one where the coupling is mediated by the charge variables [10–12].

In this work, we look at the issue from a different perspective. We use the gauge degree of freedom to find an optimal gauge such that the results of the effective model are as close as possible to full model. Importantly, we take account of the need for a multimode description [13–16] in the quest for achieving the ultra-strong coupling regime [17–20]. To increase the flexibility, we not only consider the extremal cases of purely flux or charge mediated coupling but perform a general gauge transformation that smoothly interpolates between the two. A similar transformation has been used in [21] to extend the Jaynes-Cummings model into the ultra-strong coupling regime.

We find that already the second order term of the effective Hamiltonian within the SW method is a good indicator of the validity of the QRM. Based on this observation, we derive a simple analytical criterion for the optimal gauge and benchmark it against numerical sim-

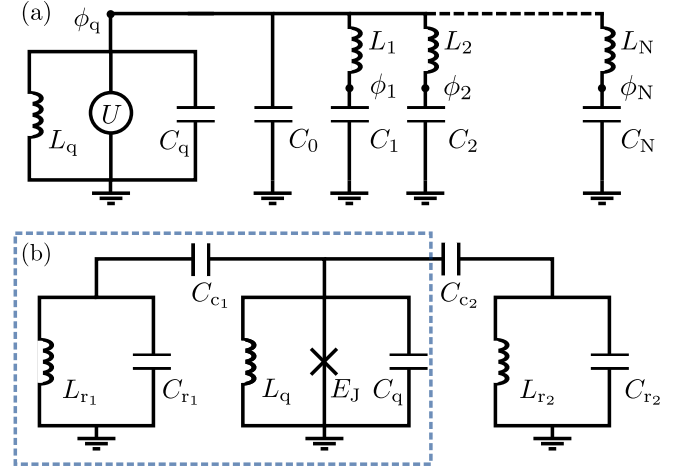


FIG. 1. (a) Circuit diagram of a qubit with potential $U(\phi_q)$, capacitance C_q , and inductance L_q that is coupled to a general reactive environment. In the Forster form, the latter is represented by N resonators with capacitances C_k and inductances L_k ($k = 1, \dots, N$). (b) Fluxonium qubit (consisting of a Josephson junction with energy E_J in parallel to the capacitance C_q and a large inductance L_q), capacitively coupled to two resonators with inductances L_{r_k} and capacitances C_{r_k} ($k = 1, 2$). In the text, the example of a single resonator (dashed box) is treated separately.

ulations of the full problem. For a qubit coupled to a single-mode resonator, the flux gauge is always the best gauge [10, 11, 19]. This serves as an analogue of the dipole gauge in quantum optics [22]. Considering more than one mode drastically changes this simple picture. The optimal gauge may now deviate from the pure flux gauge as can be demonstrated with two resonator modes. We show that this already has implications for weak to moderate coupling.

General case.—Consider a qubit consisting of an LC-oscillator in parallel with a symmetric potential $U(\phi_q)$ that is coupled to a linear, reactive environment, cf. Fig. 1(a). We denote the qubit Hamiltonian H_q and the resonator Hamiltonian H_r . They are coupled via the in-

interaction V such that the total Hamiltonian is given by $H = H_q + H_r + V$. Using the unitary freedom of the Hamiltonian formalism, we introduce a gauge parameter $\eta \in [0, 1]$ that linearly interpolates between a qubit-resonator interaction mediated by the flux variables ϕ_k (for $\eta = 0$) and the charge variables Q_k (for $\eta = 1$) [23]. We will refer to these extremal cases as the flux and the charge gauge, respectively. For a general gauge, the interaction reads

$$V(\eta) = - \sum_{k=1}^N \left[\frac{(1-\eta)\phi_q\phi_k}{L_k} + \frac{\eta Q_q Q_k}{C_\Sigma} \right] \quad (1)$$

$$+ (1-\eta)^2 \sum_{k=1}^N \frac{\phi_q^2}{2L_k} + \eta^2 \frac{\left(\sum_{k=1}^N Q_k\right)^2}{2C_\Sigma};$$

here, $C_\Sigma = C_q + C_0$ denotes the total capacitance of the qubit to ground. The first term of Eq. (1) is the analogue of the paramagnetic coupling. The second part is a diamagnetic term that renormalizes qubit and the resonator frequencies and ensures the gauge invariance of the full Hamiltonian [23, 24].

For most quantum information applications, we are interested in projecting H_q onto a subspace $S = \{|0\rangle, |1\rangle\}$ spanned by the two lowest eigenstates. To obtain an effective Hamiltonian, we apply the SW method resulting in $H_{\text{eff}} = \sum_{j=0}^K H_j$ to K -th order. The first order result $H_0 + H_1$ corresponds to the projection of H onto S . It is equivalent to the generalized QRM [23, 25]

$$H_{\text{QRM}}(\eta) = -\frac{\hbar\omega_{10}^q}{2}\sigma^z + \sum_{k=1}^N \hbar\omega_k a_k^\dagger a_k \quad (2)$$

$$+ \hbar \sum_{k=1}^N \left[(1-\eta)g_k^\phi \sigma^x (a_k + a_k^\dagger) + \eta g_k^Q \sigma^y (a_k - a_k^\dagger) \right],$$

where $\hbar\omega_{nm}^q$ is the energy difference between the n -th and the m -th eigenstate of H_q and σ^j ($j = x, y, z$) denote the Pauli operators. In Eq. (2), we have rewritten the variables of the k -th resonator mode with frequency ω_k in terms of bosonic creation operators a_k^\dagger and annihilation operators a_k . The coupling between the qubit and the k -th resonator mode is given by $g_k^\phi = \langle 1|\phi_q|0\rangle \sqrt{Z_k/2\hbar L_k^2}$ and $g_k^Q = \langle 1|Q_q|0\rangle / \sqrt{2\hbar Z_k C_\Sigma^2}$, where Z_k is the characteristic impedance of the k -th mode. In deriving Eq. (2), we neglected the diamagnetic shift due to the second term present in Eq. (1) for simplicity. For weak coupling, the diamagnetic shift is irrelevant. In general, it can be accounted for using symplectic diagonalization [26, 27].

Restricting the perturbative series of H_{eff} to any finite order necessarily results in a gauge dependent model. The source of the gauge dependence of the QRM is that the coupling between the subspace S and its orthogonal complement S^\perp is not properly taken into account in the projection. Increasing the order K weakens the gauge dependence [28, 29] at the expense of introducing a dressed

basis that results in a model that strays quite far from the natural interpretation of the QRM. In this respect, the lowest order approximation provided by the QRM is an appealing model as it yields a low-energy description without rotating the basis. In the simple effective model Eq. (2), choosing a gauge such that the QRM accurately captures the physics of the full Hamiltonian is crucial. We are thus concerned with the task of finding an optimal gauge parameter η_* such that the differences between the QRM and the full Hamiltonian are minimized.

A criterion for the optimal gauge.—To address this issue, we note that the validity of the QRM is directly proportional to the coupling strength between S and S^\perp . The higher order SW terms H_j ($j > 1$) can therefore be used as an estimator for the difference between the full model and its effective description as a QRM. Based on this observation, we derive an analytic criterion for the optimal gauge.

In particular, we focus on the second order term H_2 , which will provide the largest corrections to H_{QRM} for weak coupling. H_2 is proportional to matrix elements $V_{nm} = \langle n|V|m\rangle$ of the interaction, where $|n\rangle \in S$ and $|m\rangle \in S^\perp$. Motivated by Eq. (1), we define the paramagnetic flux coupling operator $G_k^\phi = \phi_q\phi_k^{\text{zp}}/\hbar L_k$ and the charge coupling operator $G_k^Q = Q_q Q_k^{\text{zp}}/\hbar C_\Sigma$ [30]. Here, we have approximated the resonator matrix elements by their zero point fluctuations $\phi_k^{\text{zp}} \simeq \sqrt{\hbar Z_k}$ and $Q_k^{\text{zp}} \simeq \sqrt{\hbar/Z_k}$, respectively. In order to estimate the relevance of the flux versus the charge coupling (for the transition $m \mapsto n$), we introduce the ratio $f_{nm} = [\sum_k (G_k^\phi)_{nm}] / [\sum_k (G_k^Q)_{nm}]$. Using the fact that $(Q_q)_{nm} = i\omega_{nm}^q C_\Sigma (\phi_q)_{nm}$, it can be compactly rewritten as

$$|f_{nm}| = \frac{\sum_k p_k \omega_k}{\omega_{nm}^q} = \frac{\bar{\omega}}{\omega_{nm}^q}, \quad (3)$$

where $\bar{\omega}$ is the average of the resonator frequencies ω_k with the weights $p_k = Z_k^{-1/2} / (\sum_l Z_l^{-1/2})$.

The interpretation of Eq. (3) is as follows: if $|f_{nm}| \ll 1$, the coupling between S and S^\perp in the flux gauge is much smaller than the coupling in the charge gauge. The QRM with $\eta \approx 0$ is therefore a good approximation of the full model, making the flux gauge the preferred choice. But, if $|f_{nm}| \gg 1$, the coupling of the qubit subspace to higher levels is small in the charge gauge which thus is the optimal gauge. In the intermediate regime, where $|f_{nm}| \simeq 1$, both, flux and charge variables contribute similarly to the coupling between S and S^\perp . Consequently, we expect the optimal gauge to be neither the pure charge nor the flux gauge but a mixed gauge with $\eta \neq 0, 1$.

For weak qubit-resonator interactions, the dominant contribution to H_2 will be due to the coupling of the first and second excited level of the qubit. The character of the coupling of the optimal gauge is therefore mostly determined by the ratio of the anharmonicity of the qubit

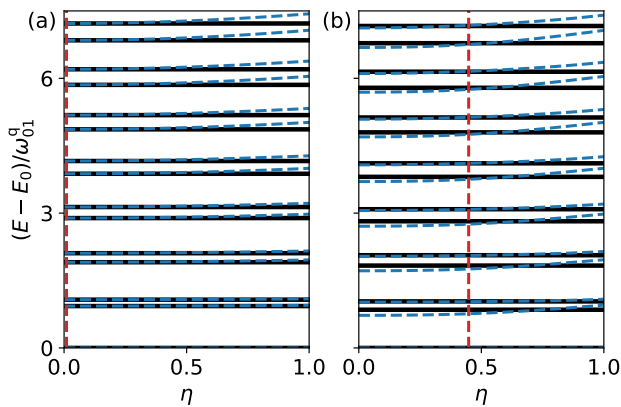


FIG. 2. Spectrum of the full Hamiltonian H (solid lines) and the Rabi model Hamiltonian H_{QRM} (dashed lines) for a fluxonium qubit coupled to a single resonator (a) and to two resonators (b). The qubit parameters are $(E_J, E_C, E_L) = \hbar(12.5, 3.75, 0.5)$ GHz, where $E_C = e^2/2C_\Sigma$ and $E_L = (\phi_0/2\pi)^2/L_q$. The resulting qubit frequency is $\omega_{10}^q = 0.5$ GHz and $\omega_{21}^q = 13$ GHz. Furthermore, $\omega_1 = \omega_{10}^q$ and $g_1^q/\omega_1 = 0.07$. In (b) the parameters of the second resonator are $C_{r_2} = C_{r_1}$, $C_{c_2} = C_{c_1}$ and $\omega_2 \approx \omega_{12}^q$ such that $\bar{\omega} = 10.7$ GHz. The value η_* that minimizes $\|H_2\|_*$ is shown as a vertical dashed line.

to an effective frequency of the linear environment. We conclude that f_{21} of Eq. (3) provides a simple estimation of the optimal coupling. It requires only knowledge of the qubit anharmonicity and the frequency and impedances of the linear environment. We illustrate these findings with two specific examples in the following.

Single resonator.—First, we consider a qubit coupled to a single resonator ($N = 1$). Note that in this case the average frequency $\bar{\omega}$ in Eq. (3) is equal to ω_1 . For the interaction between the qubit and the resonator mode to be appreciable, we assume that $\omega_1 \simeq \omega_{10}^q$. Consequently, Eq. (3) yields $|f_{21}| \simeq \omega_{10}^q/\omega_{21}^q$ and the optimal gauge is solely determined by the properties of the qubit. To reach strong coupling, the qubit has to be anharmonic with $\omega_{10}^q \ll \omega_{21}^q$ [19]. This implies $|f_{21}| \ll 1$, so we find that the flux gauge is always the optimal gauge for this case.

To demonstrate this result, we numerically study the fluxonium qubit with $E_L = (\phi_0/2\pi)^2/L_q \lesssim E_J$ and $U(\phi_q) = -E_J \cos[2\pi(\phi_q - \phi_{\text{ext}})/\phi_0]$ [31]; here, E_J is the Josephson energy, $\phi_0 = h/2e$ is the superconducting flux quantum, and ϕ_{ext} is an external magnetic flux threading the superconducting loop. We set the external flux to the degeneracy point $\phi_{\text{ext}} = \frac{1}{2}\phi_0$ which results in a symmetric potential. The qubit parameters are chosen such that the qubit is strongly anharmonic with $\omega_{21}^q/\omega_{10}^q \approx 25$ (see Fig. 2 for details). The fluxonium qubit is coupled to a parallel combination of a capacitor C_{r_1} and inductance L_{r_1} which together form a resonator with a frequency $\omega_1 = \omega_{10}^q$, cf. Fig. 1(b) (dashed box). The setup can be

mapped to the canonical Foster circuit with $N = 1$ shown in Fig. 1(a) [23].

Figure 2(a) shows the spectrum of the full Hamiltonian (solid) compared to the spectrum of H_{QRM} (dotted) as a function of η . The spectra agree well in the flux gauge ($\eta = 0$). For increasing values of η , that is for more charge-like gauges, the spectral agreement between truncated and full model decreases. The disagreement is more pronounced in levels with higher energy as they are closer to the energy of the second excited level of the qubit. We observe that f_{21} of Eq. (3) is suitable for estimating the overall tendency for being charge or flux-like. A more quantitative estimate of the optimal coupling η_* can be obtained by calculating the norm of H_2 . Based on the discussion surrounding Eq. (3), we expect that η_* is approximately the η for which the norm $\|H_2\|_*$ [32] is minimized. For the parameters in Fig. 2(a), the minimum of $\|H_2\|_*$ is at $\eta = 0$, which is shown in red (dotted) and agrees well with the visual impression conveyed by the spectrum. A quantitative analysis can be found in Ref. [23].

Two resonators.—As a second example, we treat the case where there are two relevant modes ($N = 2$). As before, the first mode is close to resonance with the qubit frequency. The second mode with frequency ω_2 can be interpreted as a parasitic mode. Since the average frequency $\bar{\omega}$ in Eq. (3) is a function of all modes coupled to the qubit, the optimal gauge is now also dependent on the parasitic mode. This is true even for strongly off-resonant modes, as the coupling to higher modes in the flux gauge increases $\propto (\omega_2)^2$ at fixed impedance, see Eq. (1). As a result, for large detuning with $\omega_2 \gg \omega_{21}^q$, the charge gauge becomes more favorable. In contrast to the single-mode case, the optimal gauge for two resonators is not determined by the properties of the qubit alone but depends on the parameters of the whole circuit.

To show this effect, we perform numerical simulations of the circuit in Fig. 1(b). The fluxonium is capacitively coupled to two parallel LC oscillators via the capacitances C_{c_1} and C_{c_2} . This circuit can be mapped to the canonical Foster circuit depicted in Fig. 1(a) [23]. Figure 2(b) shows the spectrum of the full Hamiltonian (black, solid) and the QRM (dashed, blue) as a function of η . The parameters of the qubit and the first resonator are the same as in Fig. 2(a). The frequency of the second resonator, however, is significantly larger such that $\bar{\omega} \approx \omega_{12}^q$. In contrast to the single-resonator case, the spectral lines of H and H_{QRM} do not cross at $\eta \approx 0$ but rather around $\eta \approx 0.5$, suggesting the optimal gauge does not coincide with the usual ad-hoc choices of the flux or charge gauge. This is in agreement with the prediction based on the minimization of $\|H_2\|_*$ which yields $\eta_* = 0.45$ (shown as a dashed vertical line).

The deviation between H and H_{QRM} is state dependent for finite qubit anharmonicities, a fact that we have neglected so far. As a result, the intersection of the spec-

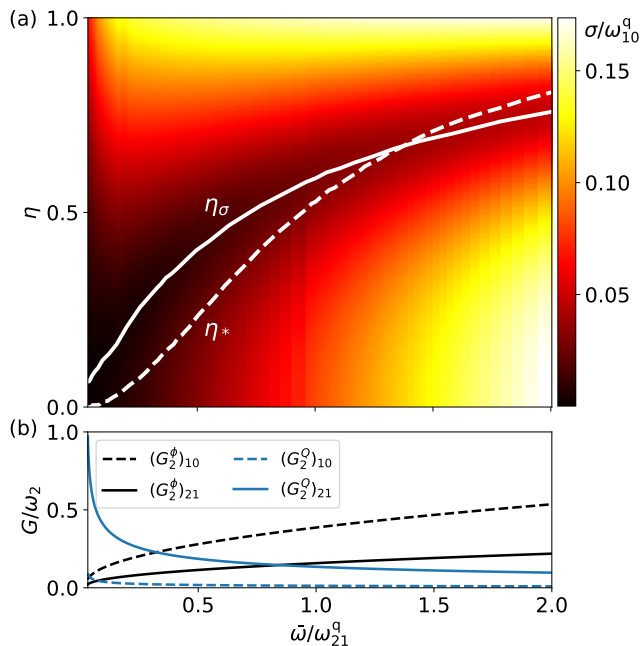


FIG. 3. (a) Deviation σ of the energy eigenvalues of the full model from the energy eigenvalues of the QRM as function of η and $\bar{\omega}$. The qubit parameters and the parameters of the first resonator are the same as in Fig. 2. The coupling capacitances to both resonators are equal $C_{c1} = C_{c2} = C_c$. The average frequency $\bar{\omega}$ is varied by changing the inductance of the second resonator L_{r2} . The value η_σ for which σ is minimized is shown in as a solid line. The value of η_* for which $\|H_2\|_*$ is minimized is shown as a dashed line. (b) Coupling strength between qubit levels n and m (see legend) as a function of $\bar{\omega}$.

tral lines of H and H_{QRM} in Fig. 2(b) is shifted towards smaller values of η for increasing energy of the levels. In the intermediate regime where $\omega_q^{21} \simeq \bar{\omega}$ ($f_{21} \simeq 1$), the optimal gauge is thus always a compromise which minimizes the differences of H and H_{QRM} in the relevant spectral range.

To demonstrate the dependence of the optimal gauge on $\bar{\omega}$, we keep the frequency ω_1 of the first mode in resonance with the qubit while varying $\bar{\omega}$. To simulate an experimentally feasible scenario, we choose the inductance L_{r2} of the second resonator as the parameter that we vary [33]. Decreasing L_{r2} while keeping all other parameters constant increases the frequency ω_2 of the parasitic mode while simultaneously decreasing its impedance. Since $\bar{\omega}$ decreases with the square root of Z_2 but increases linearly with ω_2 , the average frequency $\bar{\omega}$ grows with decreasing L_{r2} . To quantify the agreement between the full Hamiltonian and the QRM, we use the standard deviation $\sigma = [\sum_{i=0}^M (E_i - e_i)^2 / M]^{1/2}$ between the energies E_i of the full Hamiltonian and the energies e_i of the QRM (measured from the respective ground-state energy). We denote the value of η for which σ is minimized by η_σ .

Figure 3(a) shows σ as a function of $\bar{\omega}$ and η for the first

15 energy levels. We see that $\eta_\sigma \approx 0$ (flux gauge) for $\bar{\omega} \ll \omega_{10}^q$. Increasing the average frequency $\bar{\omega}$, the optimal gauge moves towards the charge gauge. Furthermore, we note that although the minimal value of σ increases with increasing $\bar{\omega}$, the overall deviation between the full model and the QRM at η_σ is only a few percent. The value η_* which minimizes $\|H_2\|_*$ is shown as a dashed line. It can be observed that η_* behaves similarly to η_σ .

To support our discussion surrounding Eq. (3), we analyze the coupling between S and S^\perp . Figure 3(b) shows $(G_2^\phi)_{nm}$ (black) and $(G_2^Q)_{nm}$ (blue) for the parameters of Fig. 3(a). In general, the charge coupling G^Q decreases while the flux coupling G^ϕ increases with increasing $\bar{\omega}$. For small values of $\bar{\omega}$, the dominant quantity is $(G_2^Q)_{21}$. This results in a large coupling between S and S^\perp in the charge gauge, making the flux gauge the preferred choice. As $\bar{\omega}$ increases, the coupling to the higher qubit levels in the charge variables decreases and eventually becomes comparable to the coupling in the flux variables, making the choice of the optimal gauge less trivial.

Conclusion.— We have analyzed the gauge dependence of the effective description of an anharmonic system coupled to a general linear environment. Using a SW transformation, we have derived a simple, analytic criterion that predicts the optimal gauge where the physics of the non-truncated Hamiltonian is accurately captured by the QRM. We have demonstrated that the optimal gauge for a qubit resonantly coupled to a single resonator is completely determined by the qubit parameters and is in the flux-like regime for strongly anharmonic qubits. We have seen that coupling a qubit to more than one mode can result in an optimal gauge that is neither the charge nor the flux gauge but a non-trivial combination of the two. This is especially relevant with the increasing interest in the ultra-strong coupling regime which raises the need for multimode descriptions.

-
- [1] Alexandre Blais, Ren-Shou Huang, Andreas Wallraff, S. M. Girvin, and R. J. Schoelkopf, “Cavity quantum electrodynamics for superconducting electrical circuits: An architecture for quantum computation,” *Phys. Rev. A* **69**, 062320 (2004).
 - [2] A Wallraff, D I Schuster, A Blais, L Frunzio, R.-S Huang, J Majer, S Kumar, S M Girvin, and R J Schoelkopf, “Strong coupling of a single photon to a superconducting qubit using circuit quantum electrodynamics,” *Nature* **431** (2004).
 - [3] Sebastian Schmidt and Jens Koch, “Circuit qed lattices: Towards quantum simulation with superconducting circuits,” *Ann. Phys.* **525**, 395–412 (2013).
 - [4] M. H. Devoret and R. J. Schoelkopf, “Superconducting circuits for quantum information: An outlook,” *Science* **339**, 1169–1174 (2013).
 - [5] G Wendin, “Quantum information processing with superconducting circuits: a review,” *Rep. Prog. Phys.* **80**,

- 106001 (2017).
- [6] J. R. Schrieffer and P. A. Wolff, “Relation between the anderson and kondo hamiltonians,” *Phys. Rev.* **149**, 491–492 (1966).
- [7] Sergey Bravyi, David P. DiVincenzo, and Daniel Loss, “Schriefferwolff transformation for quantum many-body systems,” *Ann. Phys.* **326**, 2793 – 2826 (2011).
- [8] Willis E. Lamb, “Fine structure of the hydrogen atom. iii,” *Phys. Rev.* **85**, 259–276 (1952).
- [9] Kuo-Ho Yang, “Gauge transformations and quantum mechanics i. gauge invariant interpretation of quantum mechanics,” *Ann. Phys.* **101**, 62 – 96 (1976).
- [10] Daniele De Bernardis, Philipp Pilar, Tuomas Jaako, Simone De Liberato, and Peter Rabl, “Breakdown of gauge invariance in ultrastrong-coupling cavity qed,” *Phys. Rev. A* **98**, 053819 (2018).
- [11] Daniele De Bernardis, Tuomas Jaako, and Peter Rabl, “Cavity quantum electrodynamics in the nonperturbative regime,” *Phys. Rev. A* **97**, 043820 (2018).
- [12] O. Di Stefano, A. Settineri, V. Macrì, L. Garziano, R. Stassi, S. Savasta, and F. Nori, “Resolution of gauge ambiguities in ultrastrong-coupling cavity qed,” arXiv:1809.08749 (2018).
- [13] Simon E. Nigg, Hanhee Paik, Brian Vlastakis, Gerhard Kirchmair, S. Shankar, Luigi Frunzio, M. H. Devoret, R. J. Schoelkopf, and S. M. Girvin, “Black-box superconducting circuit quantization,” *Phys. Rev. Lett.* **108**, 240502 (2012).
- [14] Firat Solgun, David W. Abraham, and David P. DiVincenzo, “Blackbox quantization of superconducting circuits using exact impedance synthesis,” *Phys. Rev. B* **90**, 134504 (2014).
- [15] A Parra-Rodriguez, E Rico, E Solano, and I L Egusquiza, “Quantum networks in divergence-free circuit QED,” *Quantum Sci. Technol.* **3**, 024012 (2018).
- [16] Fabian Hassler, Jakob Stubenrauch, and Alessandro Ciani, “Equation of motion approach to black-box quantization: Taming the multimode jaynes-cummings model,” *Phys. Rev. B* **99**, 014515 (2019).
- [17] Mario F. Gely, Adrian Parra-Rodriguez, Daniel Bothner, Ya. M. Blanter, Sal J. Bosman, Enrique Solano, and Gary A. Steele, “Convergence of the multimode quantum rabi model of circuit quantum electrodynamics,” *Phys. Rev. B* **95**, 245115 (2017).
- [18] Sal J Bosman, Mario F Gely, Vibhor Singh, Alessandro Bruno, Daniel Bothner, and Gary A Steele, “Multi-mode ultra-strong coupling in circuit quantum electrodynamics,” *npj Quantum Inf.* **3**, 46 (2017).
- [19] Vladimir E Manucharyan, Alexandre Baksic, and Cristiano Ciuti, “Resilience of the quantum rabi model in circuit QED,” *J. Phys. A* **50**, 294001 (2017).
- [20] Anton Frisk Kockum, Adam Miranowicz, Simone De Liberato, Salvatore Savasta, and Franco Nori, “Ultrastrong coupling between light and matter,” *Nat. Rev. Phys.* **1**, 19–40 (2019).
- [21] Adam Stokes and Ahsan Nazir, “Gauge ambiguities imply Jaynes-Cummings physics remains valid in ultrastrong coupling QED,” *Nat. Comm.* **10**, 499 (2019).
- [22] Claude CohenTannoudji, Jacques DupontRoc, and Gilbert Grynberg, *Photons and Atoms* (Wiley-VCH, Weinheim, 1999).
- [23] See supplementary material for details on the gauge transformation, the full Hamiltonian, the SWT, and additional numerics for the one-mode case.
- [24] Moein Malekakhlagh and Hakan E. Türeci, “Origin and implications of an A^2 -like contribution in the quantization of circuit-qed systems,” *Phys. Rev. A* **93**, 012120 (2016).
- [25] Here, the parity symmetry $U(-\phi_q) = U(\phi_q)$ is important for giving the selection rules $\langle j|Q_q|j\rangle = \langle j|\phi_q|j\rangle = 0$.
- [26] Martin Idel, Sebastian Soto Gaona, and Michael M. Wolf, “Perturbation Bounds for Williamson’s Symplectic Normal Form,” arXiv:1609.01338 (2016).
- [27] R. Simon, S. Chaturvedi, and V. Srinivasan, “Congruences and canonical forms for a positive matrix: Application to the schweinerwigner extremum principle,” *J. Math. Phys.* **40**, 3632–3642 (1999).
- [28] L S Cederbaum, J Schirmer, and H D Meyer, “Block diagonalisation of hermitian matrices,” *J. Phys. A* **22**, 2427–2439 (1989).
- [29] Y. Aharonov and C. K. Au, “Gauge invariance and pseudoperturbations,” *Phys. Rev. A* **20**, 1553–1562 (1979).
- [30] Note that the couplings G^ϕ and G^Q are generalizations of the couplings introduced in Eq. (2) such that $\langle 0|G^\phi|1\rangle = -g^\phi$ and $\langle 0|G^Q|1\rangle = -ig^Q$.
- [31] Vladimir E. Manucharyan, Jens Koch, Leonid I. Glazman, and Michel H. Devoret, “Fluxonium: Single cooper-pair circuit free of charge offsets,” *Science* **326**, 113–116 (2009).
- [32] In Figs. 2 and 3 we have used the trace norm $\|\mathcal{H}\|_* = \sum_k |\lambda_k|$ for an Hermitian operator \mathcal{H} with eigenvalues λ_k . Since we are only interested in the value of η that minimizes the norm of H_2 , other norms can be used as well.
- [33] M A Castellanos-Beltran, K D Irwin, G C Hilton, L R Vale, and K W Lehnert, *Nat. Phys.* **4**, 929 (2008).
- [34] M.H. Devoret, “Quantum fluctuations in electrical circuits,” in *Proceedings of the Les Houches Summer School, Session LXIII* (Elsevier Science B. V, New York, 1995).
- [35] Roland Winkler, *Spin-Orbit Coupling Effects in Two-Dimensional Electron and Hole System* (Springer Berlin Heidelberg, 2003) pp. 201–205.

SUPPLEMENT

GAUGE TRANSFORMATION

In this chapter, we introduce the gauge transformation discussed in the main text on a Lagrangian level. The Lagrangian $\mathcal{L}(\phi, \dot{\phi})$ of a qubit in potential U coupled to a general linear environment is a function of the fluxes $\phi = (\phi_q, \phi_1, \dots, \phi_N)^T$ and the voltages proportional to $\dot{\phi}$. Here, the dot denotes the time derivative. Using the capacitance matrix C and the inverse of the inductance matrix $M = L^{-1}$, it can be written as

$$\mathcal{L}(\phi, \dot{\phi}) = \frac{1}{2} \dot{\phi}^T C \dot{\phi} - \frac{1}{2} \phi^T M \phi - U(\phi_q). \quad (\text{S1})$$

The Euler-Lagrange equations are invariant under coordinate transformations. The choice of coordinates corresponds to choosing a specific gauge in electromagnetic field theory. In Eq. (S1), the flux variable ϕ_q is distinguished from the rest by the presence of the potential $U(\phi_q)$. We thus consider coordinate transformations $\phi = T\phi'$ that preserve this structure and leave the variable ϕ_q invariant. In its most general form, such a transformation is given by

$$T = \begin{pmatrix} 1 & \mathbf{0} \\ \mathbf{t} & R \end{pmatrix}, \quad (\text{S2})$$

where R is an invertible matrix and \mathbf{t} is an N -dimensional vector.

In general, both C and M provide a qubit-resonator coupling. In the following, we show that it is not possible to decouple the qubit from the resonator with a transformation of the form of Eq. (S2). To demonstrate this, we write C and M in the same block structure as Eq. (S2)

$$C = \begin{pmatrix} \kappa & \mathbf{c}^T \\ \mathbf{c} & C_r \end{pmatrix}, \quad M = \begin{pmatrix} \mu & \mathbf{m}^T \\ \mathbf{m} & M_r \end{pmatrix}. \quad (\text{S3})$$

Here, κ is the qubit capacitance and μ is the qubit inductance. Moreover, C_r and M_r are the capacitance and inverse inductance matrices of the resonators. The vectors \mathbf{c} and \mathbf{m} couple the flux and voltage variables of the qubit and the resonators. Under the transformation Eq. (S2), C and M transform as $C' = T^T C T$ and $M' = T^T M T$ which yields the transformed off-diagonal blocks $\mathbf{c}' = R\mathbf{c} + RC_r\mathbf{t}$ and $\mathbf{m}' = R\mathbf{m} + RM_r\mathbf{t}$. Therefore, in order for \mathbf{c}' and \mathbf{m}' to vanish at the same time, the following equations have to be satisfied

$$\mathbf{m} - M_r C_r^{-1} \mathbf{c} = 0, \quad (\text{S4})$$

$$\mathbf{c} - C_r M_r^{-1} \mathbf{m} = 0. \quad (\text{S5})$$

These equations can only be satisfied simultaneously if the qubit and the resonators are uncoupled. Nevertheless, one can choose coordinates such that the qubit is coupled to the resonator only through the capacitance or the inverse inductance matrix, respectively. In the following, we fix \mathbf{t} and introduce a gauge parameter η that linearly interpolates between these two extreme cases

$$\mathbf{t} = - [(1 - \eta)C_r^{-1}\mathbf{c} + \eta M_r^{-1}\mathbf{m}]. \quad (\text{S6})$$

One can easily verify that $\eta = 0$ results in a block-diagonal capacitance matrix C' . The coupling is then completely inductive and we call the corresponding gauge *flux gauge*. On the other hand, $\eta = 1$ block-diagonalizes M' which results in a purely capacitive coupling. We call the corresponding gauge *charge gauge*.

FULL HAMILTONIAN

Figure 1(a) in the main text shows a qubit in a potential U coupled to a general admittance modelled by a series of LC oscillators. Choosing the flux gauge to represent the circuit (determined by the choice of ground node [34]), the Lagrangian is given by

$$\mathcal{L}(\phi, \dot{\phi}) = \frac{C_\Sigma \dot{\phi}_q^2}{2} - \frac{\phi_q^2}{2L_q} - U(\phi_q) + \sum_{k=1}^N \left[\frac{C_k \dot{\phi}_k^2}{2} - \frac{(\phi_k - \phi_q)^2}{2L_k} \right]. \quad (\text{S7})$$

Here, $C_\Sigma = C_q + C_0$ is the total capacitance of the qubit to ground. We introduce a gauge parameter η by performing the variable transformation Eq. (S2) discussed in the previous section. We use the specific \mathbf{t} from Eq. (S6). For the Lagrangian in Eq. (S7) the coupling vectors read $\mathbf{c} = \mathbf{0}$ and $\mathbf{m} = (-L_1^{-1}, -L_2^{-1}, \dots, -L_N^{-1})^T$. The capacitance and inductance matrices of the resonators are diagonal. They are given by $C_r = \text{diag}(C_1, C_2, \dots, C_N)$ and $M_r = \text{diag}(L_1^{-1}, L_2^{-1}, \dots, L_N^{-1})$. Performing the transformation yields

$$\mathcal{L}'(\phi', \dot{\phi}') = \frac{C_\Sigma \dot{\phi}'_q{}^2}{2} - \frac{\phi'_q{}^2}{2L_q} - U(\phi'_q) + \sum_{k=1}^N \left[\frac{C_k (\dot{\phi}'_k + \eta \dot{\phi}'_q)^2}{2} - \frac{(\phi'_k - (1-\eta)\phi'_q)^2}{2L_k} \right], \quad (\text{S8})$$

where, $\phi = T\phi'$. We define the conjugate momenta $Q'_i = \frac{\partial \mathcal{L}'}{\partial \dot{\phi}'_i}$ of the flux variables ϕ' , and perform a Legendre transformation which yields the Hamiltonian $H = \sum_i Q'_i \dot{\phi}'_i - \mathcal{L}'$. To obtain a quantum mechanical description, we promote the canonical variables to operators $\phi'_i \rightarrow \hat{\phi}_i$ and $Q'_i \rightarrow \hat{Q}_i$, and impose the canonical commutation relation $[\hat{\phi}_i, \hat{Q}_j] = i\hbar\delta_{ij}$, where δ_{ij} is the Kronecker delta. The total Hamiltonian $H(\eta) = H_q + H_r + V(\eta)$ can then be split into a qubit Hamiltonian H_q , a resonator Hamiltonian H_r and the interaction V with

$$H_q = \frac{\hat{Q}_q^2}{2C_\Sigma} + \frac{\hat{\phi}_q^2}{2L_q} + U(\hat{\phi}_q), \quad H_r = \sum_{k=1}^N \frac{\hat{Q}_k^2}{2C_k} + \frac{\hat{\phi}_k^2}{2L_k}, \quad (\text{S9a})$$

$$V(\eta) = - \sum_{k=1}^N \left[\frac{(1-\eta)\hat{\phi}_q\hat{\phi}_k}{L_k} + \frac{\eta\hat{Q}_q\hat{Q}_k}{C_\Sigma} \right] + (1-\eta)^2 \sum_{k=1}^N \frac{\hat{\phi}_q^2}{2L_k} + \eta^2 \frac{\left(\sum_{k=1}^N \hat{Q}_k\right)^2}{2C_\Sigma}. \quad (\text{S9b})$$

The interaction V in Eq. (S9b) is given in Eq. (1) of the main text where the hats over the operators have been omitted. Note that the Hamiltonian $H(\eta)$ is related to the Hamiltonian $H(\eta')$ through the unitary transformation $R = \exp[-i(\eta' - \eta)\hat{\phi}_q \sum_k \hat{Q}_k/\hbar]$ such that $R^\dagger H(\eta)R = H(\eta')$. The difference of $H(\eta) - H(0)$ corresponds to a pseudoperturbation of Ref. [29].

SCHRIEFFER-WOLFF TRANSFORMATION

In this section, we perform a SW transformation to derive the QRM Eq. (2). Similar to the main text, we define the low energy subspace of the qubit $S = \{|0\rangle, |1\rangle\}$ and its orthogonal complement S^\perp . Furthermore, we define the projector $P = |0\rangle\langle 0| + |1\rangle\langle 1|$ onto S . The projector onto S^\perp is then given by $Q = 1 - P$. The coupling between the subspaces S and S^\perp is provided by PVQ . Performing a SW transformation to block-diagonalize H with respect to S and S^\perp results in an effective Hamiltonian $H_{\text{eff}} = \sum_{j=0}^K H_j$ [35]. The zeroth order is given by the projection of the uncoupled Hamiltonian onto S

$$H_0 = PH_qP + H_r = -\hbar \frac{\omega_{10}^q}{2} \sigma^z + \hbar \sum_{k=1}^N \omega_k a_k^\dagger a_k. \quad (\text{S10})$$

Here, $\hbar\omega_{10}^q$ is the energy difference between the ground state and the first excited state of the qubit. Furthermore, we have defined the frequencies $\omega_k = 1/\sqrt{L_k C_k}$ and the bosonic raising and lowering operators of the k -th mode

$$\hat{\phi}_n = \sqrt{\frac{\hbar Z_k}{2}} (a_k^\dagger + a_k), \quad (\text{S11})$$

$$\hat{Q}_k = i\sqrt{\frac{\hbar}{2Z_k}} (a_k^\dagger - a_k), \quad (\text{S12})$$

where $Z_k = \sqrt{L_k/C_k}$ is the characteristic impedance of the k -th mode. The next order is given by the projection of the interaction V onto S

$$H_1 = PV(\eta)P = \hbar \sum_{k=1}^N \left[(1-\eta)g_k^\phi \sigma^x (a_k + a_k^\dagger) + \eta g_k^Q \sigma^y (a_k - a_k^\dagger) \right] - \frac{(1-\eta)\alpha}{2} \sigma^z - \frac{\eta^2 \hbar}{2C_\Sigma} \left(\sum_{k=1}^N \frac{a_k^\dagger - a_k}{\sqrt{Z_k}} \right)^2, \quad (\text{S13})$$

where $g_k^\phi = \langle 1|\phi_q|0\rangle\sqrt{Z_k/2\hbar L_k^2}$ and $g_k^Q = \langle 1|Q_q|0\rangle/\sqrt{2\hbar Z_k C_\Sigma^2}$. Furthermore, $\alpha = (\langle 1|\phi_q^2|1\rangle - \langle 0|\phi_q^2|0\rangle)\sum_n 1/L_n$. The last two terms in Eq. (S13) are diamagnetic renormalizations of the qubit and resonator frequencies. If these terms are omitted, the first order effective Hamiltonian $H_0 + H_1$ is equal to the QRM Eq. (2) in the main text. For weak qubit-resonator coupling this is a reasonable assumption.

FOSTER REPRESENTATION

The circuit shown in Fig. 1(b) can be mapped onto the general Foster form of Fig. 1(a). Assuming a symmetric coupling $C_{c_1} = C_{c_2} = C_c$, the capacitances and inductances are given by the following substitutions

$$C_k = \frac{C_c^2}{C_c + C_{r_k}} \quad L_k = \frac{L_{r_k}(C_c + C_{r_k})^2}{C_c^2}, \quad (\text{S14})$$

with

$$C_0 = \frac{C_c C_{r_1}}{C_c + C_1}, \quad (\text{S15})$$

for the one-mode setup (dashed box) and

$$C_0 = C_c \left(\frac{C_{r_1}}{C_c + C_{r_1}} + \frac{C_{r_2}}{C_c + C_{r_2}} \right), \quad (\text{S16})$$

for the two-mode setup.

SINGLE RESONATOR RESULTS, DETAILED

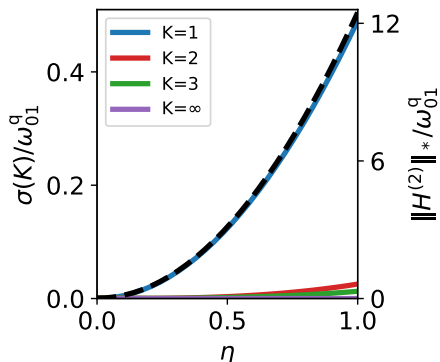


FIG. S1. Standard deviation σ of the full spectrum and the effective Hamiltonian H_{eff} to K -th order. The QRM corresponds to $K = 1$ (blue). Moreover $K = 2$ (red), $K = 3$ (green) and the exact SW transformed Hamiltonian $K = \infty$ (purple) are shown. Additionally, the norm $\|H_2\|_*$ of the first perturbative correction to H_{QRM} is shown (black, dashed). The parameters are the same as in Fig. 2 in the main text.

In this section, we show supporting data for one qubit coupled to one resonator. Figure S1 shows the standard deviation $\sigma(K) = \sqrt{(1/M)\sum_{i=0}^M (E_i - e_i(K))^2}$ for the first 15 states. Note that here $e_i(K)$ denote the eigenvalues of the SW transformed Hamiltonian H_{eff} to K -th order. In Fig. S1, the parameters are the same as in Fig. 2 in the main text. For all finite values of K , the minimum of σ is at $\eta \approx 0$ demonstrating that the flux gauge is optimal in this case.

Furthermore, we see that adding higher order terms to the Rabi Hamiltonian mitigates the effect of the broken gauge invariance. The deviation between full and effective model becomes less sensitive to variations in η with increasing order in the SW method. The exact SW transformation [28] (purple) results in a gauge invariant two-level description. Additionally, the norm of H_2 is shown (black, dashed). We observe a non-linear increase towards charge-like gauges as expected from the previous discussion. For $K = 1$ (blue, solid), we see a strikingly similar functional dependence on η as in $\|H_2\|_*$, indicating that a large part of the corrections to H_{QRM} are already captured by H_2 .